Research Article

For reprint orders, please contact: reprints@futuremedicine.com

Epigenomics

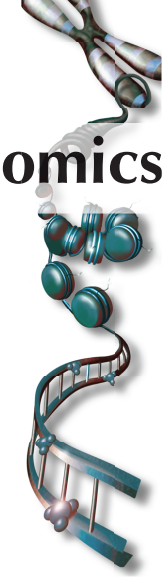

The upregulation of hypoxia-related miRNA 210 in primary tumor of lymphogenic metastatic prostate cancer

Okyaz Eminaga*[,1,2], Jochen Fries[3], Susanne Neiß[4], Michaela Heitmann[4], Fabian Wötzel[5], Axel Heidenreich[1], Christiane Bruns[4], Hakan Alakus[4] & Ute Warnecke-Eberz[4]

[1]Department of Urology, University Hospital of Cologne, Kerpenerstr. 62, D-50937 Cologne, Germany

[2]Department of Urology, Stanford University, Stanford, CA 94305, USA

[3]Department of Pathology, University Hospital of Cologne, Kerpenerstr. 62, D-50937 Cologne, Germany

[4]Laboratory for Molecular Oncology, University Hospital of Cologne, Kerpener Strasse 62, D-50937 Cologne, Germany

[5]Department of Pathology, University Hospital of Muenster, Albert-Schweitzer-Campus 1, D- 48149 Muenster, Germany

*Author for correspondence: Tel.: +49 221 478 82108; okyaz.eminaga@gmail.com

Aim: To show the association between the expression level of hsa-miR-210 (miR-210) and tumor progression in prostate cancer (PCa). **Methods:** Quantitative PCR was performed to measure miR-210 on 55 subjects with different tumor stages; our results were then validated using three external datasets. ANOVA and Tukey's *post hoc* analysis were performed for comparative analyses between different tumor stages. Using the transcriptome data from The Cancer Genome Atlas for CaP, the gene expression analyses were performed on experimentally validated target genes of miR-210 identified in Tarbase and miRWalk datasets. **Results & conclusion:** miR-210 was significantly higher in N1 PCa compared with nonmetastatic PCa, whereas the metastatic tumor revealed a lower expression level of miR-210 than the primary tumor.

First draft submitted: 11 September 2017; Accepted for publication: 19 December 2017; Published online: 15 August 2018

Keywords: metastases • microRNA • prostate cancer

Prostate cancer (PCa) is one of the most frequently diagnosed cancers and the third leading cause of death from cancer among men worldwide [1]. Current diagnostics, screening and treatment optimization are ineffective to determine PCa with metastasis potential in early stages [2,3]. Therefore, new biomarkers are required for PCa that inherits the metastasis potential. Hypoxia in cancer seems to be a consequence of the growth of a malignant tumor and may promote tumor development; hypoxic conditions in solid malignancies may further cohere with resistance to conventional therapies and are associated with a poorer prognosis [4–6]. In PCa, several studies underlined the role of hypoxia in tumor progression and treatment response in CaP [7–10].

miRNAs are small (~22 nucleotide), noncoding RNA molecules involved in post-transcriptional regulation of gene expression acting by translational repression or degradation of targeted transcripts [11]. Specific miRNAs have been found to regulate a variety of critical processes in tumor physiology including the tumor response to hypoxia [12]. miR-210 has been identified to be directly regulated by the hypoxia induced factor (HIF) pathways [5]. miR-210 expression in tissues has further become a robust marker for tumor hypoxia and shown an association with the tumor progression in breast cancers, renal cell carcinoma, head and neck cancers [4–6,13,14]. In Pearson correlation coefficient (PC) specifically, miR-210 has been found overexpressed in tumor tissue [15], in the blood of a subset of patients with metastasis [16]. However, an association between the expression of miR-210 and disease progression in PCa remains unclear. Therefore, the current study aims to evaluate the association between the expression of miR-210 and the tumor progression in CaP.

Materials & methods

The workflow of the current study consists of four steps to evaluate the association between miR-210 and tumor stages: first, we analyzed the expression levels of miR-210 in different tumor stages to evaluate the expression changes as the tumor progresses. Second, we evaluated the expression changes between metastatic and nonmetastatic CaP.

Future Medicine

Third, we compared the expression levels between the primary tumor and the corresponding loco-regional lymph node metastases. For all recent steps, we utilized external datasets to validate our results. Finally, we performed *in silico*-analyses of genes that are experimentally proven to be associated with miR-210.

Sample acquisition

Eighty-nine formalin fixed paraffin-embedded (FFPE) samples of prostatectomy specimens of 55 patients, who were treated at University Hospital Cologne between 2004 and 2015, were randomly selected based on the tumor stage of PCa to collect samples represent different stages of adenocarcinoma of the prostate. All patients, whose samples were considered for the current study, underwent prostatectomy with extended lymph node dissection and did not receive any neoadjuvant therapy. Seventeen of these specimens had high-grade prostatic intraepithelial neoplasia (HGPIN). Additional three FFPE-tissues of three cases with castration-resistant PCa (CRPC) obtained from the palliative transurethral resection were enrolled in our study. These specimens of primary tumors were divided into six groups by the tumor progression: noncancer involved prostatic tissues (n = 17); HGPIN (n = 20), organ-confined PCa (n = 20); locally advanced PCa (n = 12); lymphogenic metastatic pN1 PCa (n = 20); and CRPC (n = 3). Organ-confined PCa was defined as PCa with pT2 tumor stage and Gleason score $\leq$7 and prostate-specific antigen (PSA) level $<$10 ng/ml. PCa with pT3/4 was defined as advanced PCa. pN1 PCa were considered as lymphogenic metastatic PCa. Furthermore, ten lymph nodes having extended metastasis ($>$70% of the lymph node) and corresponding matched normal tissues were selected from ten different cases of the lymphogenic metastatic PCa group. Lymph nodes with metastases formed the group 'lymph node metastases' and were compared with the corresponding primary tumors.

All cases with HGPIN were reviewed three-times by three different independent, experienced pathologists to avoid the interobserver variability. The regions of interest, including PCa or HGPIN $>$90%, were marked on H&E slides under microscopic observation by a single pathologist. Informed consent was obtained from all patients, and the regulation of the Helsinki declaration was followed. Ethical approval for analysis of samples and notes was obtained from the local research ethics committee (IBR: 14335).

Isolation of total RNA from paraffin-embedded tissue

Tissue samples were stained by hematoxylin and evaluated for the location of the tumor area by a staff pathologist. Macro-dissection was done with 15 tissue slices of 4-µm thickness. In total, 60–80 µm of paraffin-embedded tissue specimen were used for RNA extraction. The tissue samples were prepared for RNA extraction by mixing for 3 min in 320 µl of deparaffinization solution at 56°C, with the addition of 240 µl of PKD buffer and 10 µl of proteinase K (Qiagen, Hilden, Germany). miRNA was isolated using miRNeasy FFPE Kit (Qiagen) by following the instructions of the manufacturer. miRNA was eluted with elution buffer and yielded 12 µl of 200–800 ng of miRNA per microliter.

Reverse transcription

A total of 10 ng of total RNA have been reverse-transcribed into cDNA by TaqMan microRNA RT kit (Life Technologies, Darmstadt, Germany), using 3 µl of specific primer miR-210–3p or snoU6-specific microRNA primers, respectively, adding 7 µl Mastermix, and scaling up to 15 µl of RT end volume. RT was performed by following the instruction provided by the manufacturer.

Quantitative real-time PCR

Expression of miR-210-3p and snoU6 was quantified by TaqMan7900HT (Life Technologies), snoU6 expression was used as a calibrator. TaqMan microRNA Assays applied were hsa-miR-210–3p ID000512, and snoU6 ID001973 as an internal control. One microliter containing 1 ng of cDNA was used in each of the 20 µl of real-time PCR assays. Real-time PCR quantification of miR-210–3p was carried out in triplicates by following the recommendation of the manufacturer.

External validation

We selected three publicly accessible datasets (GEO: GSE21036 [17], ArrayExpress: E-TABM-794 [18], and The Cancer Genome Atlas-Prostate Adenocarcinoma: TCGA-PRAD). These datasets provide miRNA-expression profiles, the pathologic tumor stage, and the lymph node status for PCa. miRNA reads per million data from TCGA-PRAD were transformed and normalized using the standard score as previously described [19]. Additionally, miRNA ex-

Table 1. The miR-210–3p expression levels for each tumor progression stage (p-value for ANOVA test).

Sample type	Sample, n	Quantity miR-210-3p, mean (95% CI)	Transformed miR-210-3p, mean (95% CI)
Normal	17	9.16 (7.59–10.72)	3.13 (2.90–3.36)
HGPIN	20	8.43 (7.10–9.76)	3.02 (2.81–3.23)
Organ-confined	20	5.70 (4.39–7.00)	2.40 (2.08–2.72)
Locally advanced	12	7.35 (5.49–9.21)	2.78 (2.40–3.16)
Metastatic disease	20	10.15 (7.65–12.66)	3.16 (2.81–3.51)
Lymph node metastases	10	5.26 (3.74–8.39)	2.28 (1.90–3.06)
CRCP	3	13.11 (9.71–17.1)	3.67 (3.28–4.09)
p-value		<0.001	<0.001

CRCP: Castration; HGPIN: High-grade prostatic intraepithelial neoplasia.

pression profiles of lymph node metastasis of PCa were available from datasets 'GSE21036' and 'E-TABM-794'. After quantile normalization and logic transformation of miRNA datasets, we evaluated the expression levels of miR-210 after stratifying the sample collection by lymph node status (N0 vs N1) from 'GSE21036' dataset. The expression levels of miR-210 were further compared between primary tumor and lymph node metastasis using 'E-TABM-794' dataset.

In silico analysis

We evaluated the expression data of 1054 miRNAs from TCGA-PRAD after stratifying the sample collection by lymph node status (N0 vs N1). The evaluation of expression data was done using differential gene expression analysis based on the negative binomial distribution (DESeq2) [20]. In parallel, we used Diana-web tool with Tarbase [21], miRWalk [22], Reactome pathway analysis [23], and cBioPortal [24] to identify and evaluate experimentally validated target genes and pathways related to miR-210. The expression and the copy number variation (CNV) of the targets genes were evaluated in TCGA-PRAD database. The global normalization was performed, and the row counts were transformed as already described by [25]. The somatic CNV of target genes was evaluated using GISTIC as already described elsewhere [25]. The Pearson correlation was employed to evaluate the association between gene expression and miR-210 expression. The Spearman or Pearson correlations were applied to investigate three associations – in other words, between gene expression and tumor progression, gene expression and CNV; as well as between CNV and miR-210 expression. The χ^2 test was used to determine the variation of CNV after stratifying the TCGA samples into organ-confined PCa, advanced PCa and metastatic PCa.

Statistical analysis

The expression level of miR-210-3p was normalized by using the geometric mean of the endogenous control snoU6 and log-transformed. ANOVA and *post hoc* analysis (Tukey) were performed. All statistical analysis was performed using the R statistical package system (R Foundation for Statistical Computing, Vienna, Austria) and SPSS 23 (IBM, NY, USA). One thousand bootstraps samples were applied to reduce the overfitting and for internal validation. The student's t-test was applied to compare the expression level of miR-210-3p between primary tumor and lymph node metastasis and between N0 and N1 PCa. All the statistical tests were two-sided, and the level of statistical significance was set at $p < 0.05$. Furthermore, p-values were adjusted using the false discovery rate (FDR) for multiple comparisons.

Results

The specimen characteristic is described in Supplementary Table 1. The expression level of miR-210-3p was evaluated in normal tissues, HGPIN and tumor tissues at different tumor stages. The ANOVA test and *post hoc* analysis revealed a significant association between miR-210-3p expression and tumor progression (Table 1 & Figure 1). miR-210-3p was significantly upregulated in metastatic PCa and castration-resistant prostate cancer (CRCP) in comparison to organ-confined PCa. However, no significant differences between organ-confined and locally advanced PCa have been observed (FDR = 0.534). Furthermore, no significant differences in miR-210 expression between normal tissue/HGPIN and locally advanced, lymphogenic metastatic PCa or CRPC have been detected. When the population with PCa was divided by the lymph node status, miR-210 was up-regulated in pN1 PCa (log fold change [FC]: 1.52; 95% CI: 1.22–2.07; FDR = 0.01) (Figure 2). When the samples were stratified

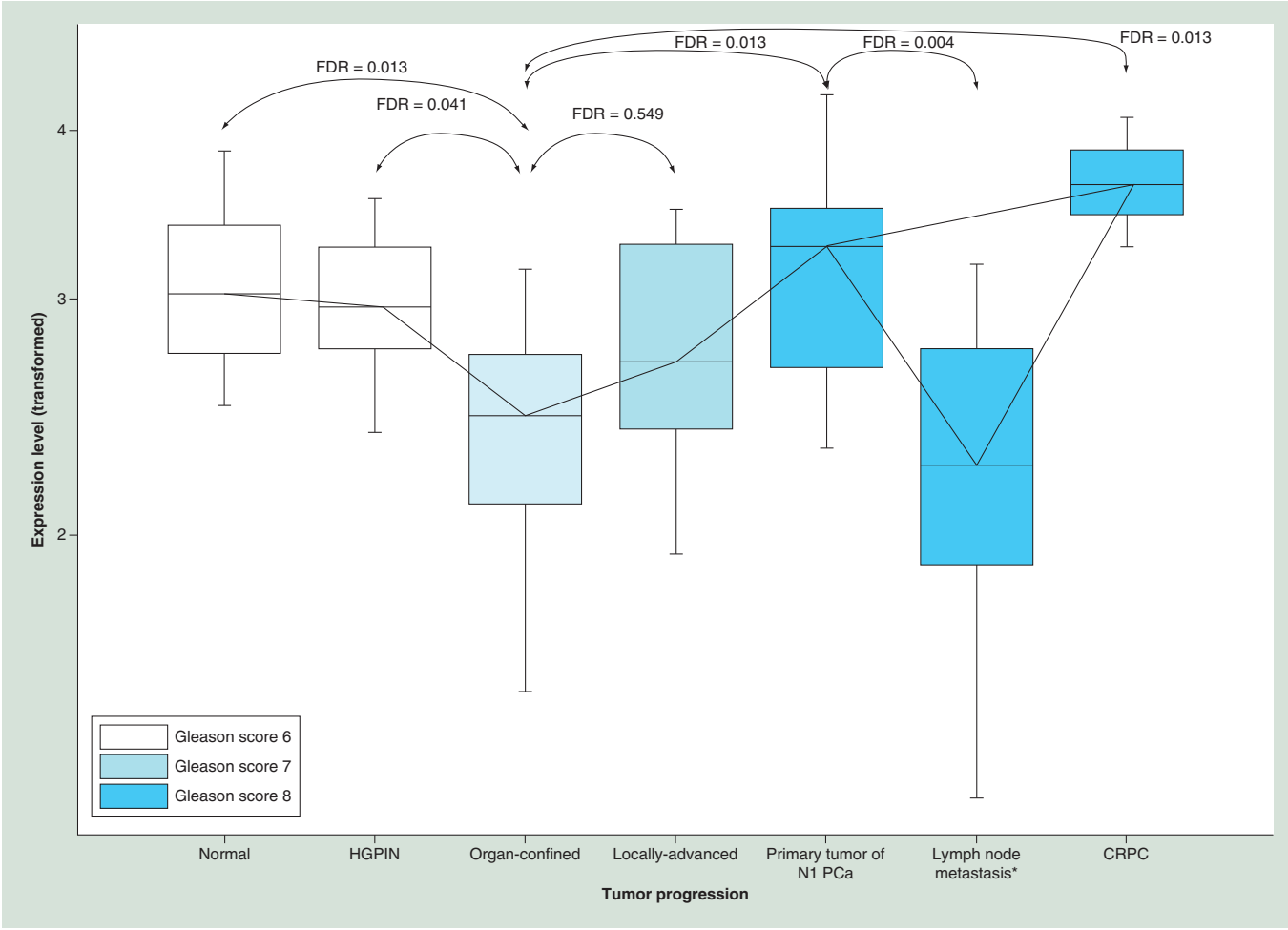

Figure 1. A box plot showing the expression levels of miR-210-3p in the primary tumor of prostate cancer representing different tumor stages. The results of *post hoc* analysis revealed a significant association between miR-210-3p expression and tumor progression. The color of the box represents the Gleason score.
†Denotes that the samples were from the metastatic sites of prostate cancer.
FDR: False discovery rate.

by Gleason score to identify the association between Gleason score and miR-210 (Figure 3); the expression level of miR-210 was higher in Gleason scores 8–9 compared with that in Gleason score 6 (FC: 1.22; 95% CI: 1.21–1.28; FDR = 0.023). However, the expression of miR-210 was similar between Gleason score 6 and 7 (FC: 1.08; 95% CI: 1.00–1.17; FDR = 0.55). Overall, the correlation of miR-210 with Gleason score was weak but significant (Spearman correlation [SC]: 0.361, FPR = 0.0109).

When comparing the expression levels of miR-210-3p between lymph node metastasis and the primary tumor of N1 PCa, miR-210-3p was lower in metastatic tissues compared with that in primary tumors of N1 PCa (FC: 0.55; 95% CI: 0.30–0.60; FDR = 0.004). To see whether the decrease in miR-210 associated with a contamination of normal tissues, we compared the expression level between lymph node metastases and matched normal tissues. Here, we found that miR-210–3p was highly expressed in lymph node metastases compared with matched normal lymph node tissues (FC: 1.39; 95% CI: 1.03–1.64; FDR = 0.04).

Our results were validated by using external datasets. Based on expression analysis of TCGA dataset, we identified that miR-210 was significantly upregulated (FC:1.42; 95% CI: 1.21–6.7; FDR < 0.001) in lymphogenic metastatic disease (n = 75) compared with N0 PCa (n = 254) (Figure 4). No significant difference in miR-210 expression was found between organ-confined PCa (n = 17) and locally advanced PCa (n = 237). In addition, we repeated our analysis on cases with organ-confined PCa (n = 51) having a risk of lymph node metastasis lesser than 1% and N1 PCa (n = 5) from the dataset 'GSE21036'; the expression level of miR-210 was higher in N1 PCa compared

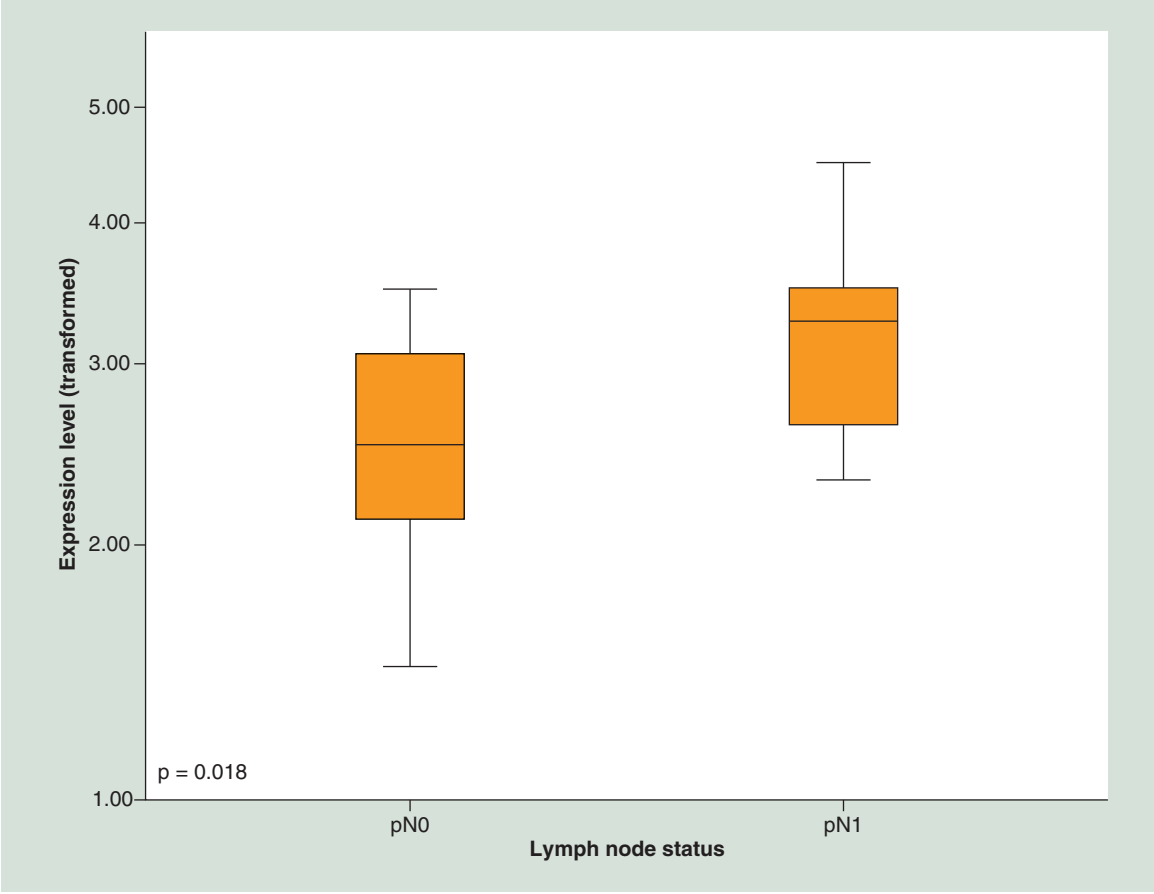

Figure 2. A box plot shows the expression level of miR-210-3p between lymphogenic metastatic and nonmetastatic prostate cancer.

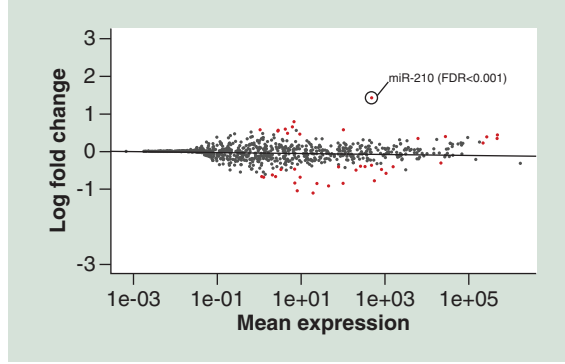

Figure 3. The results of differential gene expression analysis based on the negative binomial distribution (Deseq2) and the expression data of 1054 miRNAs from The Cancer Genome Atlas dataset, when the population was stratified according to lymph node status (N0 vs N1). The expression level of miR-210 was identified with a log fold change of 1.4 in N1 PCa compared with N0 PCa.

with organ-confined PCa (FC: 1.11; 95% CI: 1.08–1.14; FDR < 0.001) (Figure 5). Moreover, we considered the external dataset 'E-TABM-794' to validate the expression level of miR-210 in metastatic tissues, which included lymph node metastases (n = 12) and primary tumor of PCa (n = 72). miR-210 was slightly but significantly lower in lymph node metastases in comparison to that in primary tumors (FC: 0.98; 95% CI: 0.96–0.99; FDR = 0.04) (Figure 6).

We have utilized the TCGA dataset to evaluate the expression level of hypoxia-related genes (i.e., HIF1A, HIF3A, CA9, VHL, EGLN1–3, VEGFA, JUN, CREBBP, EP300 and FGFRL1) in different tumor stages (i.e., organ-confined, locally advanced PCa and lymphogenic metastatic PCa) (Supplementary Table 2). We identified that the expression level of HIF3A, a direct target of miR-210, was inversely correlated with tumor progression

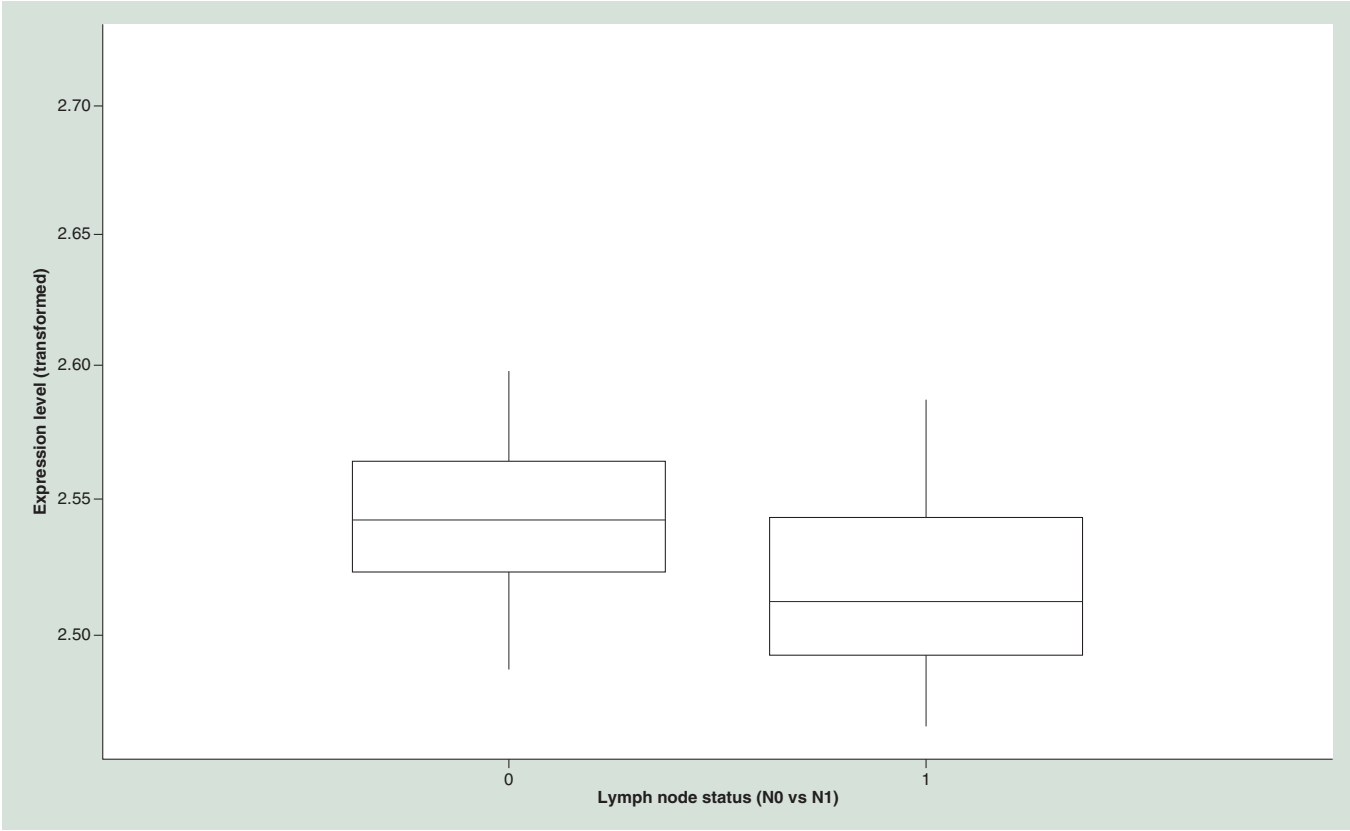

Figure 4. A box plot shows the expression levels of miR-210 according to the lymph node status. Here, we used the dataset 'E-TABM-794' to validate our result.

(SC: -0.50; FDR <0.0001). The expression level of FGFR1 was correlated with the tumor progression (SC: 0.46; FDR <0.0001). However, both genes were weakly but significantly correlated with miR-210 (PC): -0.26, FDR <0.0001 for HIF3A; PC: 0.21; FDR <0.0001 for FGFR1).

In silico analysis

Identification & gene set enrichment analysis of target genes regulated by miR-210

Supplementary Table 3 lists and describes validated target genes regulated by miR-210. The pathway analysis shows that these genes are involved in the regulation of mitotic cell cycle phase transition, the regulation of cell cycle phase transition, ephrin receptor activity, the activity of transmembrane receptor protein tyrosine kinase, homologous recombination and nonhomologous end-joining.

GSEA analysis reveals that chromatin remodeling, cell cycle, DNA replication, chromosome maintenance and homologous recombination and double-strand break repair were significantly upregulated in N1 PCa in comparison to N0 PCa (Supplementary Table 4). Despite that, genes related to glutathione conjugation, peptide chain elongation, metabolism of steroid hormones and vitamins A and D, biological oxidations and platelet calcium homeostasis were significantly enriched in N0 PCa in comparison to N1 PCa. When we focused on pathways and biological processes related to target genes, these biological processes were significantly altered between N1 and N0 PCa (Table 2). The correlation analysis identified possible interactions between target genes and MYC or TP53, which play a role in cell cycle progression, apoptosis and cellular transformation. The interaction of target genes with significantly correlated genes is illustrated in Supplementary Figure 1.

Copy number variation & expression of target genes

The alteration analysis revealed that 95% of cases with N1 PCa had a genetic alteration (i.e., CNV: 53%, gene expression: 95% and mutation: 6%) of target genes. Contrastingly, 87% of cases with N0 PCa had a genetic alteration (CNV: 41%, gene expression: 79% and mutation 10%).

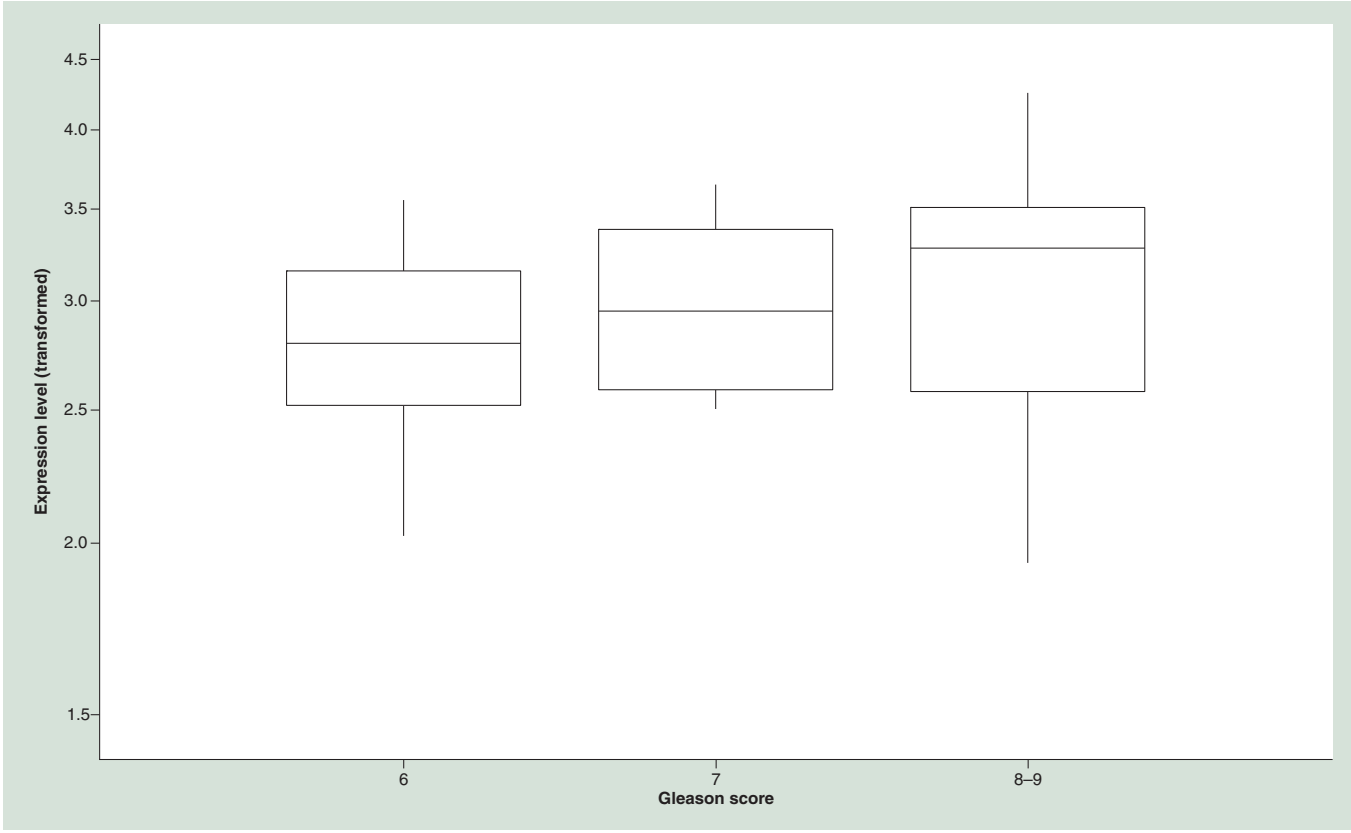

Figure 5. A box plot shows the expression levels of miR–210–3p for different Gleason scores.

Table 2. The pathways and biological processes of target genes.

Reactome pathways	Rank	Total number of genes	Number of target genes	Adj. p-value	Symbols of traget genes
Cell cycle	0.0746	473	8	0.0002	*SEH1L, ACTR1A, ESPL1, RCC2, NIPBL, CLASP2*
Cell cycle, mitotic	0.0622	394	7	0.0005	*SEH1L, ACTR1A, ESPL1, RCC2, NIPBL, CLASP2*
M phase	0.0349	221	5	0.0013	*SEH1L, ESPL1, RCC2, NIPBL, CLASP2*
Separation of sister chromatids	0.0240	152	4	0.0024	*SEH1L, ESPL1, RCC2, CLASP2*
Mitotic anaphase	0.0252	160	4	0.0029	*SEH1L, ESPL1, RCC2, CLASP2*
Mitotic metaphase and anaphase	0.0254	161	4	0.0029	*SEH1L, ESPL1, RCC2, CLASP2*
Resolution of sister chromatid cohesion	0.0144	91	3	0.0048	*SEH1L, RCC2, CLASP2*
Mitotic prometaphase	0.0156	99	3	0.0060	*SEH1L, RCC2, CLASP2*
Developmental biology	0.0743	471	6	0.0070	*EFNA3, ACVR1B, NCAM1, SCN1B, CHD9, CLASP2*
Transport of mature mRNA derived from an intron-containing transcript	0.0080	51	2	0.0159	*U2AF2, SEH1L*
Transport of mature transcript to cytoplasm	0.0087	55	2	0.0183	*U2AF2, SEH1L*

The biological processes were significantly altered between N1 and N0 prostate cancer.
Adj.: Adjusted.

The expression level of miR-210 was significantly correlated with genes related to ephrin receptor signaling pathway, positive regulation of IGF receptor signaling pathway, TNF-α/NF-kB signaling pathway, mRNA splicing, chromatin remodeling, chromosome segregation, positive regulation of cell cycle phase transition and Notch signaling pathway (Supplementary Table 4). These genes were upregulated in lymphogenic metastasis compared with

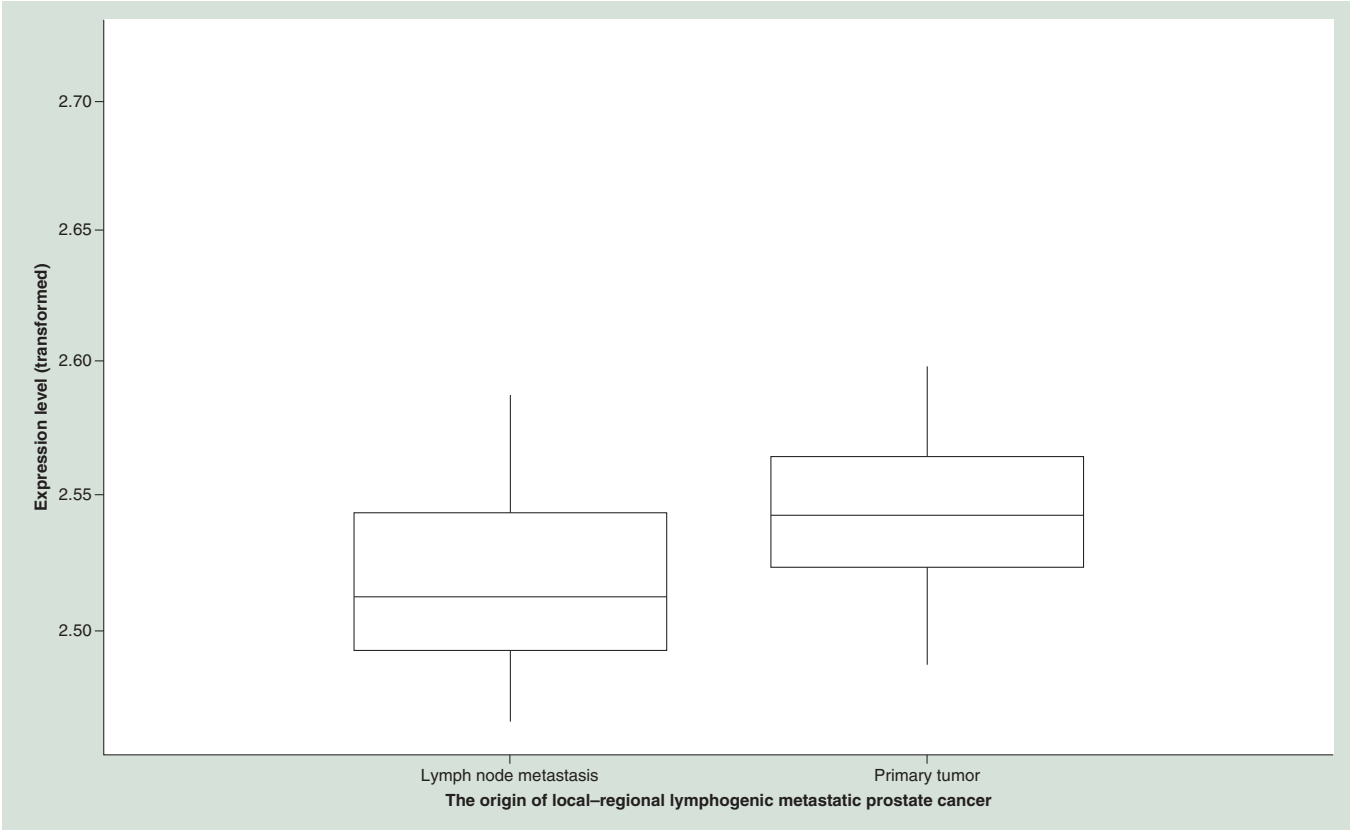

Figure 6. A box plot shows the expression levels of miR-210 in the primary and metastatic tumor of prostate cancer. Here, we used the dataset 'GSE21036' to validate our result.

those in organ-confined PCa. In contrast, the expression level of miR-210 was significantly inversely correlated with genes related to FGF signaling pathway, BDNF signaling pathway, Notch signaling pathway, ERK signaling, and negative regulation of HIF-pathway those were not methylated. These genes were downregulated in lymphogenic metastasis compared with those in organ-confined PCa. Furthermore, we observed an increase in the frequency of CNV with the tumor progression (Table 3). However, no significant correlation between CNV frequency and miR-210 expression was observed (FDR $>$ 0.05).

Discussion

The current study evaluated the expression of hypoxia-related miR-210 in different tumor stages and precursor of PCa. When we compared the expression level of miR-210 between N0 PCa and N1 PCa, expression of miR-210 was significantly higher in N1 PCa in comparison to N0 PCa. This observation could be confirmed by independent datasets [17,18]. Interestingly, we identified for the first time the variability of miR-210-3p expression according to tumor progression. Further, the expression level of miR-210-3p was lowest in early-stage organ-confined PCa below the expression level of normal and HGPIN tissues imposing the downregulation of miR-210-3p in early-stage PCa. The reason for downregulation of miR-210-3p in early-stage PCa remains to be elucidated as there is an association between HIF-1/2 and androgen receptor, which is critical for PCa development [26,27].

A previous miRNA expression profiling study revealed that miR-210-3p is upregulated in PCa compared with normal tissues [28]. The result of the previous study is contradictory to our results due to the composition of the cohorts of the previous study that included CRCP as miR-210 is upregulated in CRPC. Our results have namely revealed that the expression of miR-210-3p depends on the tumor progression. Therefore, we emphasize the consideration of tumor progression when defining the sample cohort.

Another study found that miR-210 is upregulated in a metastatic PCa xenograft line compared with a non-metastatic CaP xenograft line derived from one patient [29], which is also in contradiction to our results presumably due to the xenograft condition. In our study, the expression of miR-210 was two-times lower in metastatic lymph

Table 3. The frequency of copy number variation and expression levels (transformed) of some target genes significantly altered according to the tumor progression.

Gene	Correlation with miR-210 level†	Orang-confined		Locally advanced		Metastatic disease		FDR	
		17 (5.2)¶		237 (72.0)¶		75 (22.8)¶			
		Expression (95% CI), transformed	CNV (%)	Expression (95% CI), transformed	CNV (%)	Expression (95% CI), transformed	CNV (%)	Expression‡	CNV§
MIB1	Inverse	-0.05 (-0.34–0.25)	11.8	0.02 (-0.06 to 0.09)	19.8	-0.07 (-0.20–0.06)	36.5	<0.001	0.022
CPEB2	Inverse	-0.30 (-0.70–0.09)	0.0	-0.19 (-0.28 to -0.10)	10.5	-0.27 (-0.42 to -0.12)	25.7	<0.001	0.022
ESPL1	Correlated	-3.30 (-3.72 to -2.88)	0.0	-2.34 (-2.50 to -2.18)	8.4	-1.83 (-2.11 to -1.55)	24.3	<0.001	0.047
FGFR1	Correlated	0.64 (0.36–0.92)	0.0	1.21 (1.09–1.32)	8.9	1.32 (1.09–1.55)	28.4	<0.001	0.014
CDK10	Correlated	0.24 (-0.16–0.64)	23.5	-0.03 (-0.13–0.08)	42.6	-0.12 (-0.28–0.03)	55.4	0.001	0.050
RAD52	n.s.	-0.25 (-0.46 to ·0.04)	0.0	-0.14 (-0.20 to -0.08)	17.3	-0.17 (-0.30 to -0.05)	36.5	0.784	0.032
ACTR1A	n.s.	0.14 (-0.05–0.32)	5.9	-0.01 (-0.05–0.04)	17.3	-0.03 (-0.12 to -0.06)	35.1	0.205	0.021
XPA	n.s.	0.56 (0.41–0.70)	0.0	0.42 (0.37–0.46)	13.5	0.51 (0.41–0.60)	37.8	0.07	0.008
E2F3	n.s.	-1.30 (-1.52 to -1.07)	8.9	-0.85 (-0.93 to -0.77)	11.8	-0.65 (-0.80 to -0.49)	24.3	<0.001	<0.001
PTPN1	n.s.	-0.13 (-0.27–0.01)	0.0	-0.14 (-0.20 to-0.09)	6.3	0.01 (-0.09–0.12)	27.0	0.042	0.002
UBQLN1	n.s.	0.01 (-0.16–0.18)	0.0	0.12 (0.08–0.16)	13.1	0.19 (0.10–0.27)	35.1	0.15	0.011
MDGA1	n.s.	-0.41 (-0.89–0.06)	5.9	-0.30 (-0.44 to -0.17)	8.4	-0.11 (-0.50–0.23)	20.3	0.204	0.005
NIPBL	n.s.	-0.33 (-0.57 to -0.10)	5.9	-0.16 (-0.22 to -0.10)	9.3	-0.10 (-0.20 to -0.01)	24.3	0.002	0.027
PIM1	n.s.	-0.16 (-0.57–0.26)	5.9	-0.33 (-0.45 to -0.21)	7.2	-0.06 (-0.39–0.27)	20.3	0.089	<0.001
CASP8AP2	n.s.	-0.53 (-1.08–0.03)	23.5	-0.35 (-0.46 to -0.24)	39.2	-0.38 (-0.65 to -0.11)	51.4	<0.001	0.029
PTAR1	n.s.	-0.47 (-0.73 to -0.21)	0.0	-0.15 (-0.22 to -0.08)	12.2	-0.02 (-0.14–0.10)	32.4	0.018	0.023
TNPO1	n.s.	-0.06 (-0.31–0.19)	5.9	0.09 (0.03 to -0.16)	23.2	0.01 (-0.11–0.13)	36.5	0.038	0.010

†The correlation was estimated by the Spearman's correlation.
‡ANOVA.
§χ^2.
¶Sample, n (%).
CNV: Copy number variation; FDR: False discovery rate; n.s.: Not significant.

node tissues than in primary metastatic tumors possibly due to co-expression of miR-210 in prostatic stroma or due to the biological conditions of PCa. However, a strong difference between primary tumors and metastatic lymph node tissues could not be seen in an external microarray dataset likely due to differences in experimental and analytical approaches, which are known to alter the experimental results [30]. As a consequence, further investigation is required to verify our assumption under comparable conditions.

Recent studies found that hypoxic senescent fibroblasts promote PCa aggressiveness by inducing epithelial to mesenchymal transition (EMT) and by secreting energy-rich compounds to support cancer cell growth [31–33]. Overexpression of the hypoxia-induced miR-210 in young fibroblasts intensify their senescence-associated features and transforms them into cancer-associated fibroblast-like cells, able to promote cancer cells EMT, to support angiogenesis and to recruit endothelial precursor cells and monocytes/macrophages [33]. Andersen *et al.* identified that the overexpression of miR-210 in fibroblasts is independently associated with poor survival [34]. Our data reveal that N1 PCa has higher Gleason score than N0 PCa, which is comparable with recent findings [24,25]. Moreover, we identified an association between miR-210-3p and Gleason score. The structural disbalance between stroma and epithelial components of PCa is getting more obvious for stroma with increasing Gleason score [35]. Interestingly, the expression level of miR-210 was lower in organ-confined prostate tumors than that in normal tissues. However, the expression levels of miR-210 between normal tissues and locally advanced or lymphogenic metastatic PCa were comparable. The expression level of miR-210 was similar between organ-confined PCa and lymph node metastases. These observations presumably depend on the biologic conditions of PCa that dynamically change during the tumor progression (e.g., hypoxia status and the proportion of the epithelial tissue and the stroma in the prostatic tissues).

Our findings imply the role of the hypoxia-related pathway in tumor progression of PCa. Quero *et al.* identified miR-210 as an interesting marker of chronic hypoxia for PCa [36]. The expression of miR-210 is regulated by HIF-1α [4,37]. Under normoxic conditions, the expression of miR-210 has been determined at low levels in

tissues [12,37]. Chang *et al.* emphasized that a positive feedback loop involving miR-210 and HIF-1α is essential for human mesenchymal stem cells' survival under hypoxic conditions [38]. Additionally, miR-210 inhibits the prolyl-hydroxylases or Succinate Dehydrogenase Complex Subunit D (SDHD), which induces the degradation or inhibition of HIF-1α, resulting in enhanced levels and stabilization of HIF-1α [12,39]. A VHL mutation results in insufficient HIF-1α degradation leading to an increase in HIF-1α levels, and a hypoxic response during normoxic conditions [13,40]. The presence of elevated miR-210 expression in tissues has become a predictive marker for hypoxia in tumor tissues inclusive PCa [36,41,42].

The TCGA dataset for PCa reveals an inverse correlation between miR-210 and HIF3A, although we did not identify significant changes in HIF-1α levels expression in different tumor stages. HIF3A is known to function as a negative regulator of hypoxia-inducible gene expression [43] and directly regulated by miR-210–3p [44]. Further, HIF3A was inversely correlated with tumor progression (i.e., organ-confined to metastatic disease). These findings underline the possible role of the negative regulators of hypoxia in tumor progression of PCa.

miR-210 overexpression may cause disturbances in the control mechanism of the cell cycle leading to multipolar spindles and excessive amplification of centrosomes presumably due to HIF1-α accumulation [45]. Moreover, Rothe *et al.* reported that overexpression of miR-210 in breast cancer cell treated with the chemotherapeutic agent Tamoxifen resulted in enhanced cell proliferation and associated with poor prognosis [6].

Ding *et al.* revealed that miR-210 promoted ovarian cancer cell mobility by acting as a modulator of EMT [46]. Cells exposed to hypoxic conditions are disposed to genetic instability and increased rates of genetic variation resulting in DNA mismatch repair [47]. Experimental evidence in support of this miR-210-induced effect revealed that tumor cells overexpressing miR-210 exhibited higher levels of double-strand DNA breaks than cells with normal levels of miR-210 [5].

The FGFR1 is ectopically expressed in PCa cells and associated with metastasis potential of PCa [48]. The TCGA dataset revealed an association between FGFR1 and tumor progression or miR-210 suggesting the importance of interaction between fibroblast cells and PCa cells for tumor progression. Although FGFRL1 was a putative target of miR-210 by high-throughput analyses, an additional epigenetic change would be existed, which should be explained in a further study.

In summary, our study underscores the potential role of miR-210 and hypoxia-related pathways in tumor progression of PCa. The current study includes a unique cohort of patients who underwent extended lymph node dissection during the radical prostatectomy. The extended lymph node dissection yields more frequently positive lymph nodes than the limited lymph node dissection and reduces the risk of false-negative N0 PCa [49].

Our study has some limitations that warrant mention. First, the heterogeneity of PCa inside the prostate may influence the expression of miR-210-3p. Nevertheless, our results could be validated using an external dataset. We did not perform specific analysis on cancer stroma. Therefore, no direct statement can be made regarding the expression of miR-210 in cancer stroma. The tumor size may have an influence on hypoxia status, and we do believe the tumor stage and aggressiveness measured by lymph node metastasis status and Gleason score represent more the tumor progression than tumor volume as recent works have shown that the predictive value of tumor volume for tumor progression is controversial [50–52]. Second, most HGPIN foci were distant from the primary tumor. Consequently, it is not feasible to evaluate whether the expression of miR-210-3p differs in HGPIN foci per distance to primary tumors. Third, the sample size is low for certain subgroup. For these reasons, we performed an external validation to verify our results. Further, the effect sizes from some comparison analyses were small to moderate, which should be considered when evaluating our results. Fourth, the external datasets are generated by microarray or sequencing-based techniques, where our data were generated by using qPCR-analyses. This variation in applied techniques leads to the alteration in measurements of miRNA levels and as consequence limits the comparative analyses. The definition of the FC cutoff is a controversial issue in the genomic data analysis. The cutoff for FC is arbitrary defined and may not necessarily represent the upregulation or downregulation of miR-210 over tumor stages. Given the applied analysis methods, the definition of FC should be opted by the kind of the scientific question [53]. Seventh, we did not consider the 5-p arm mature of hsa-miR-210-5p as the 3-p arm mature of hsa-miR-210 is identified to be associated with PCa and in hypoxia [36,41,42]. Finally, the current high-throughput miRNA expression data from TCGA and other datasets lack information regarding the expression of both the 5p-arm and 3p-arm mature miRNAs as the miRNA annotations do not include comprehensive 5p-arm/3p-arm feature annotations [54]. Another major limitation of TCGA dataset is the low number of low-risk PCa. Moreover, the completeness of clinical data are moderate, and 165 cases were excluded from our analyses due to missing clinical data (i.e., PSA, Gleason score). For our analyses, we defined organ-confined PCa as PCa with pT2pN0,

Gleason score ≤7a (3 + 4) and PSA level <10 ng/ml, which represents the lowest risk for tumor progression. Given this definition, only 17 cases met these criteria. The low number of organ-confined (early-staged) PCa does limit the comparison analysis (17 vs 237 or 75). Therefore, we considered focusing on pathologic N Status for TCGA dataset (254 vs 75), although the TCGA cohort mostly underwent radical prostatectomy and had a clinical lymph node status (cN). cN is less accurate to represent the real N status and harbor a higher risk for lymphogenic metastasis than the pathologic lymph node status in advanced PCa. Moreover, the pathologic N status in the TCGA dataset mostly originated from cases underwent the limited lymph node dissection which is another limitation of the TCGA dataset.

Conclusion

The expression of miR-210 was significantly higher in the primary tumor of PCa with lymph node metastases (N1 PCa) in comparison to that of nonmetastatic PCa. Moreover, miR-210-3p was considerably lower in lymph node metastases compared with primary tumors in the prostate of N1 PCa presumably due to the biological conditions and the proportion of epithelial and stroma parts in PCa. However, further investigation is required to verify this assumption. Our results support the potential role of miR-210 and hypoxia-related pathways in tumor progression of PCa.

Summary points

- hsa-miR-210–3p is recognized as hypoxia marker in tumor tissues.
- Our study underscores the potential role of miR-210 and hypoxia-related pathways in tumor progression of prostate cancer (PCa).
- miR-210–3p was significantly higher in N1 cancer compared with nonmetastatic PCa.
- The lymphogenic metastatic tumors revealed a lower expression level of miR-210 than the primary tumor.
- The expression level of miR-210-3p was lowest in early-stage organ-confined PCa below the expression level of normal and high-grade prostatic intraepithelial neoplasia tissues imposing the downregulation of miR-210-3p in early-stage PCa.
- *In silico* analyses, we identified that the expression level of HIF3A, a direct target of miR-210, was inversely correlated with tumor progression.
- One reason for the contradictory results of studies on miR-210 in PCa is the dependency of expression of miR-210–3p on the tumor progression.
- Our study underscores the potential role of miR-210 and hypoxia-related pathways in tumor progression of PCa.

Supplementary data

To view the supplementary data that accompany this paper please visit the journal website at: https://www.futuremedicine.com/doi/suppl/10.2217/epi-2017-0114

Financial & competing interests disclosure

The project was funded by Köln Fortune from the medical faculty of the University of Cologne. O Eminaga received a scholarship from Werner Jackstädt-Foundation. The authors have no other relevant affiliations or financial involvement with any organization or entity with a financial interest in or financial conflict with the subject matter or materials discussed in the manuscript apart from those disclosed.

No writing assistance was utilized in the production of this manuscript.

References

Papers of special note have been highlighted as: • of interest; •• of considerable interest

1. Jemal A, Siegel R, Xu J, Ward E. Cancer statistics, 2010. *CA Cancer J. Clin.* 60(5), 277–300 (2010).
2. Braillon A, Dubois G. Re: Fritz H. Schroder, Jonas Hugosson, Sigrid Carlsson, *et al.* Screening for prostate cancer decreases the risk of developing metastatic disease: findings from the European Randomized Study of Screening for Prostate Cancer (ERSPC). *Eur. Urol.* 62(5), e89; author reply e90–81 (2012).
3. Budaus L, Isbarn H, Tennstedt P *et al.* Risk assessment of metastatic recurrence in patients with prostate cancer by using the Cancer of the Prostate Risk Assessment score: results from 2937 European patients. *BJU Int.* 110(11), 1714–1720 (2012).

4. Camps C, Buffa FM, Colella S *et al.* hsa-miR-210 Is induced by hypoxia and is an independent prognostic factor in breast cancer. *Clin. Cancer Res.* 14(5), 1340–1348 (2008).
5. Gee HE, Ivan C, Calin GA, Ivan M. HypoxamiRs and cancer: from biology to targeted therapy. *Antioxid. Redox Signal.* 21(8), 1220–1238 (2014).
6. Rothe F, Ignatiadis M, Chaboteaux C *et al.* Global microRNA expression profiling identifies miR-210 associated with tumor proliferation, invasion and poor clinical outcome in breast cancer. *PLoS ONE* 6(6), e20980 (2011).
7. Marignol L, Rivera-Figueroa K, Lynch T, Hollywood D. Hypoxia, notch signalling, and prostate cancer. *Nat. Rev. Urol.* 10(7), 405–413 (2013).
8. Higgins LH, Withers HG, Garbens A *et al.* Hypoxia and the metabolic phenotype of prostate cancer cells. *Biochim. Biophys. Acta.* 1787(12), 1433–1443 (2009).
9. Marignol L, Coffey M, Lawler M, Hollywood D. Hypoxia in prostate cancer: a powerful shield against tumour destruction? *Cancer Treat Rev.* 34(4), 313–327 (2008).
10. Ammirante M, Shalapour S, Kang Y, Jamieson CA, Karin M. Tissue injury and hypoxia promote malignant progression of prostate cancer by inducing CXCL13 expression in tumor myofibroblasts. *Proc. Natl Acad. Sci. USA* 111(41), 14776–14781 (2014).
11. Flynt AS, Lai EC. Biological principles of microRNA-mediated regulation: shared themes amid diversity. *Nat. Rev. Genet.* 9(11), 831–842 (2008).
12. Nallamshetty S, Chan SY, Loscalzo J. Hypoxia: a master regulator of microRNA biogenesis and activity. *Free Radic. Biol. Med.* 64, 20–30 (2013).
13. Neal CS, Michael MZ, Rawlings LH, Van Der Hoek MB, Gleadle JM. The VHL-dependent regulation of microRNAs in renal cancer. *BMC Med.* 8, 64 (2010).
14. Gee HE, Camps C, Buffa FM *et al.* hsa-mir-210 is a marker of tumor hypoxia and a prognostic factor in head and neck cancer. *Cancer* 116(9), 2148–2158 (2010).
15. Mezlini AM, Wang B, Deshwar A, Morris Q, Goldenberg A. Identifying cancer specific functionally relevant miRNAs from gene expression and miRNA-to-gene networks using regularized regression. *PLoS ONE* 8(10), e73168 (2013).
16. Cheng HH, Mitchell PS, Kroh EM *et al.* Circulating microRNA profiling identifies a subset of metastatic prostate cancer patients with evidence of cancer-associated hypoxia. *PLoS ONE* 8(7), e69239 (2013).

•• **Evaluates the expression level of different miRNA including miR-210 in a subset of metastatic prostate cancer (PCa) patients. Moreover, they found that serum miR-210 levels varied widely among mCRPC patients undergoing therapy, and correlated with treatment response as assessed by change in PSA. Their data are important to confirm the results of our study that shows the overexpression of miRNA in metastatic PCa compared with nonmetastatic PCa.**

17. Taylor BS, Schultz N, Hieronymus H *et al.* Integrative genomic profiling of human prostate cancer. *Cancer Cell* 18(1), 11–22 (2010).

•• **Made an integrative analysis covering miRNA, gene expression profiles and genomic alteration in PCa. Their data confirmed the upregulation of miR-210 in metastatic PCa compared with nonmetastatic PCa.**

18. Martens-Uzunova ES, Jalava SE, Dits NF *et al.* Diagnostic and prognostic signatures from the small non-coding RNA transcriptome in prostate cancer. *Oncogene* 31(8), 978–991 (2012).
19. Goldman M, Craft B, Swatloski T *et al.* The UCSC cancer genomics browser: update 2015. *Nucleic Acids Res.* 43(Database issue), D812–D817 (2015).
20. Love MI, Huber W, Anders S. Moderated estimation of fold change and dispersion for RNA-seq data with DESeq2. *Genome Biol.* 15(12), 550 (2014).
21. Vlachos IS, Paraskevopoulou MD, Karagkouni D *et al.* DIANA-TarBase v7.0: indexing more than half a million experimentally supported miRNA:mRNA interactions. *Nucleic Acids Res.* 43(Database issue), D153–D159 (2015).
22. Dweep H, Gretz N, Sticht C. miRWalk database for miRNA-target interactions. *Methods Mol. Biol.* 1182, 289–305 (2014).
23. Vastrik I, D'Eustachio P, Schmidt E *et al.* Reactome: a knowledge base of biologic pathways and processes. *Genome Biol.* 8(3), R39 (2007).
24. Gao J, Aksoy BA, Dogrusoz U *et al.* Integrative analysis of complex cancer genomics and clinical profiles using the cBioPortal. *Sci. Signal.* 6(269), pl1 (2013).
25. Mermel CH, Schumacher SE, Hill B, Meyerson ML, Beroukhim R, Getz G. GISTIC2.0 facilitates sensitive and confident localization of the targets of focal somatic copy-number alteration in human cancers. *Genome Biol.* 12(4), R41 (2011).
26. Boddy JL, Fox SB, Han C *et al.* The androgen receptor is significantly associated with vascular endothelial growth factor and hypoxia sensing via hypoxia-inducible factors HIF-1a, HIF-2a, and the prolyl hydroxylases in human prostate cancer. *Clin. Cancer Res.* 11(21), 7658–7663 (2005).
27. Heinlein CA, Chang C. Androgen receptor in prostate cancer. *Endocr. Rev.* 25(2), 276–308 (2004).
28. Porkka KP, Pfeiffer MJ, Waltering KK, Vessella RL, Tammela TL, Visakorpi T. MicroRNA expression profiling in prostate cancer. *Cancer Res.* 67(13), 6130–6135 (2007).

29. Watahiki A, Wang Y, Morris J *et al.* microRNAs associated with metastatic prostate cancer. *PLoS ONE* 6(9), e24950 (2011).
30. Ioannidis JP. Non-replication and inconsistency in the genome-wide association setting. *Hum. Hered.* 64(4), 203–213 (2007).
31. Doldi V, Callari M, Giannoni E *et al.* Integrated gene and miRNA expression analysis of prostate cancer associated fibroblasts supports a prominent role for interleukin-6 in fibroblast activation. *Oncotarget* 6(31), 31441–31460 (2015).
32. Walter BA, Valera VA, Pinto PA, Merino MJ. Comprehensive microRNA profiling of prostate cancer. *J. Cancer* 4(5), 350–357 (2013).
33. Taddei ML, Cavallini L, Comito G *et al.* Senescent stroma promotes prostate cancer progression: the role of miR-210. *Mol. Oncol.* 8(8), 1729–1746 (2014).
34. Andersen S, Richardsen E, Moi L *et al.* Fibroblast miR-210 overexpression is independently associated with clinical failure in prostate cancer – a multicenter (*in situ* hybridization) study. *Sci. Rep.* 6, 36573 (2016).
35. Epstein JI, Allsbrook WC Jr, Amin MB, Egevad LL, Committee IG. The 2005 International Society of Urological Pathology (ISUP) Consensus Conference on Gleason Grading of Prostatic Carcinoma. *Am. J. Surg. Pathol.* 29(9), 1228–1242 (2005).
36. Quero L, Dubois L, Lieuwes NG, Hennequin C, Lambin P. miR-210 as a marker of chronic hypoxia, but not a therapeutic target in prostate cancer. *Radiother. Oncol.* 101(1), 203–208 (2011).
37. Huang X, Ding L, Bennewith KL *et al.* Hypoxia-inducible mir-210 regulates normoxic gene expression involved in tumor initiation. *Mol. Cell* 35(6), 856–867 (2009).
38. Chang W, Lee CY, Park JH *et al.* Survival of hypoxic human mesenchymal stem cells is enhanced by a positive feedback loop involving miR-210 and hypoxia-inducible factor 1. *J. Vet. Sci.* 14(1), 69–76 (2013).
39. Gorospe M, Tominaga K, Wu X, Fahling M, Ivan M. Post-transcriptional control of the hypoxic response by RNA-binding proteins and microRNAs. *Front. Mol. Neurosci.* 4, 7 (2011).
40. Valera VA, Walter BA, Linehan WM, Merino MJ. Regulatory effects of microRNA-92 (miR-92) on *VHL* gene expression and the hypoxic activation of miR-210 in clear cell renal cell carcinoma. *J. Cancer* 2, 515–526 (2011).
41. Ying Q, Liang L, Guo W *et al.* Hypoxia-inducible microRNA-210 augments the metastatic potential of tumor cells by targeting vacuole membrane protein 1 in hepatocellular carcinoma. *Hepatology* 54(6), 2064–2075 (2011).
42. Hwang HW, Baxter LL, Loftus SK *et al.* Distinct microRNA expression signatures are associated with melanoma subtypes and are regulated by HIF1A. *Pigment Cell Melanoma Res.* 27(5), 777–787 (2014).
43. Hara S, Hamada J, Kobayashi C, Kondo Y, Imura N. Expression and characterization of hypoxia-inducible factor (HIF)-3alpha in human kidney: suppression of HIF-mediated gene expression by HIF-3alpha. *Biochem. Biophys. Res. Commun.* 287(4), 808–813 (2001).
44. Agrawal R, Pandey P, Jha P, Dwivedi V, Sarkar C, Kulshreshtha R. Hypoxic signature of microRNAs in glioblastoma: insights from small RNA deep sequencing. *BMC Genomics* 15 686 (2014).
45. Nakada C, Tsukamoto Y, Matsuura K *et al.* Overexpression of miR-210, a downstream target of HIF1alpha, causes centrosome amplification in renal carcinoma cells. *J. Pathol.* 224(2), 280–288 (2011).
46. Ding L, Zhao L, Chen W, Liu T, Li Z, Li X. miR-210, a modulator of hypoxia-induced epithelial–mesenchymal transition in ovarian cancer cell. *Int. J. Clin. Exp. Med.* 8(2), 2299–2307 (2015).
47. Crosby ME, Kulshreshtha R, Ivan M, Glazer PM. microRNA regulation of DNA repair gene expression in hypoxic stress. *Cancer Res.* 69(3), 1221–1229 (2009).
48. Yang F, Zhang Y, Ressler SJ *et al.* FGFR1 is essential for prostate cancer progression and metastasis. *Cancer Res.* 73(12), 3716–3724 (2013).
49. Touijer K, Rabbani F, Romero Otero J, Secin F, Guillonneau B. Extended vs. limited laparoscopic pelvic lymph node dissection for prostate cancer: the value of Partin tables in selection of the need for and the extent of dissection. *J. Clin. Oncol.* 24(18 Suppl.), 4654 (2006).
50. Merrill MM, Lane BR, Reuther AM, Zhou M, Magi-Galluzzi C, Klein EA. Tumor volume does not predict for biochemical recurrence after radical prostatectomy in patients with surgical Gleason score 6 or less prostate cancer. *Urology* 70(2), 294–298 (2007).
51. Tretiakova MS, Wei W, Boyer HD *et al.* Prognostic value of Ki67 in localized prostate carcinoma: a multi-institutional study of >1000 prostatectomies. *Prostate Cancer Prostatic Dis.* 19(3), 264–270 (2016).
52. Hinkelammert R, Eminaga O, Bettendorf O *et al.* Tumor percentage but not number of tumor foci predicts disease-free survival after radical prostatectomy especially in high-risk patients. *Urol. Oncol.* 32(4), 403–412 (2014).
53. Dalman MR, Deeter A, Nimishakavi G, Duan ZH. Fold change and p-value cutoffs significantly alter microarray interpretations. *BMC Bioinformatics* 13(Suppl. 2), S11 (2012).
54. Kuo WT, Su MW, Lee YL *et al.* Bioinformatic interrogation of 5p-arm and 3p-arm specific miRNA expression using TCGA datasets. *J. Clin. Med.* 4(9), 1798–1814 (2015).